Dalton Transactions

ROYAL SOCIETY OF CHEMISTRY

PAPER

View Article Online
View Journal | View Issue

Cite this: *Dalton Trans.*, 2022, 51, 14150

Distinct modes of Si–H binding to Rh in complexes of a phosphine-diarylamido-silane (SiNP) pincer ligand†

A. Rain Talosig,[a] Mario N. Cosio,[b] Benjamin Morse,[a] Vinh T. Nguyen,[b] Alex J. Kosanovich,[b] Christopher J. Pell,[b] Chun Li,[a] Nattamai Bhuvanesh,[b] Jia Zhou,*[c] Anna S. Larsen*[a] and Oleg. V. Ozerov*[b]

Received 6th July 2022,
Accepted 24th August 2022

DOI: 10.1039/d2dt02175g

rsc.li/dalton

Syntheses of Rh complexes of the phosphine-amido-silane SiNP ligand are reported. The reaction of the parent (SiNP)H ligand (4) with 0.5 equiv. $[(COE)RhCl]_2$ (COE = *cis*-cyclooctene) in the presence of $NaN(SiMe_3)_2$ resulted in the formation of (SiNP)Rh(COE) (5). Compound 5 was converted to a series of (SiNP)$Rh(P(OR)_3)$ complexes 6–10 (R = Ph, ^{i}Pr, ^{n}Bu, Et, or Me) by treatment with the corresponding phosphite. NMR and XRD structural data, as well as the DFT computational analysis indicate that compounds 5–10 are divided into two structural Types (A and B), differing in the nature of the interaction of the Si–H bond of the SiNP ligand with Rh.

Introduction

The fundamental aspects of an interaction between a silicon-hydrogen bond and a transition metal center have attracted considerable attention as one of the key examples of the dichotomy between a classical silyl/hydride structure and a non-classical Si–H σ-complex (Fig. 1).[1,2,3] The interest in these species is especially strong owing to their relevance to catalytic hydrosilylation[4–6] and C–H silylation reactions.[7] We have been interested in the use of an Si–H functionality as a component of polydentate, pincer-type[8,9] ligands. While the Si–H containing precursors have been used to construct complexes of silyl-containing polydentate ligands,[10,11] the use of a silane site (Si–H) in polydentate ligand design is not common.

Several years ago, we disclosed that Ir complexes supported by the SiNN ligands are capable catalysts for dehydrogenative borylation of terminal alkynes (Fig. 1).[12] We analysed how the Si–H side arm in the Ir[13] and Rh[14] complexes of the SiNN ligand (*e.g.*, 1 and 2) can modulate between a σ-complex and a silyl/hydride structure, ostensibly facilitating lower-barrier reactions at the catalytically active Ir center.[15] We were interested in examining an analogous situation where the Si–H unit would maintain a σ-complex structural motif. We selected the SiNP ligand[16] and decided to pair it up with monovalent Rh carrying an additional phosphite ligand (Scheme 1). The SiNP ligand is derived from the widely studied PNP ligand,[17,18] such as in compound 3 (Fig. 1),[19] *via* formal replacement of a $-P^iPr_2$ arm with an $-SiH^iPr_2$ arm. This combination offered more NMR spectroscopic information that the previously studied

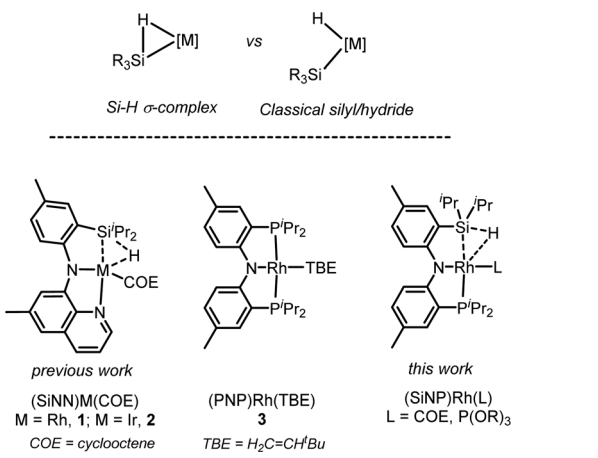

Fig. 1 Top: the two extremes of a continuum of interactions of an R_3Si–H bond with a transition metal. Bottom: the previously reported complexes of the SiNN and PNP pincer ligands, along with the SiNP complexes studies in this work.

[a]*Department of Chemistry and Biochemistry, Ithaca College, Ithaca New York, 14850, USA. E-mail: alarsen@ithaca.edu*
[b]*Department of Chemistry, Texas A&M University, TAMU – 3255, College Station, TX 77842, USA. E-mail: ozerov@chem.tamu.edu*
[c]*State Key Laboratory of Urban Water Resource and Environment, School of Science, Harbin Institute of Technology, Shenzhen 518055, China. E-mail: jiazhou@hit.edu.cn*

† Electronic supplementary information (ESI) available: Graphical NMR data and details of X-ray structure solution. CCDC 1894481 and 2033844. For ESI and crystallographic data in CIF or other electronic format see DOI: https://doi.org/10.1039/d2dt02175g

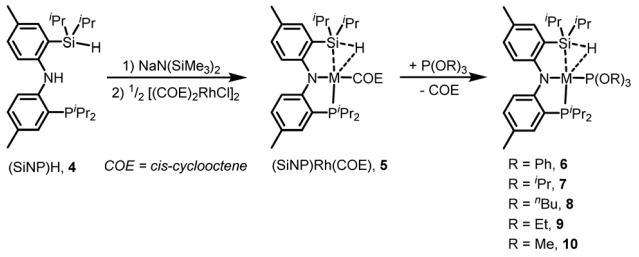

Scheme 1 Synthesis of (SiNP)Rh complexes 5–10.

(SiNN)Ir/Rh systems and we also surmised that a monovalent Rh center may not completely rupture the Si–H bond.

We set out to examine a series of comparable complexes; however, instead of a single gradual trend in the spectroscopic properties, we were faced with an apparent bifurcation of the series into two distinct types. The present report details our analysis of this situation that suggests two distinct modes of binding of the Si–H unit in the SiNP pincer complexes.

Results and discussion

Synthesis and spectroscopic characterization

Treatment of (SiNP)H (1) with $NaN(SiMe_3)_2$, followed by a reaction with 0.5 equiv. of $[(COE)_2RhCl]_2$ in fluorobenzene led to the formation of a dark red solution along with the presumed precipitate of NaCl. (SiNP)Rh(COE) (5) was isolated after filtration and workup in 50% yield as a bright-orange solid. Compound 5 gave rise to C_1-symmetric ^1H and $^{13}C\{^1H\}$ NMR spectra, and a lone doublet $^{31}P\{^1H\}$ NMR resonance. The J_{P-Rh} value in this compound (193 Hz) is considerably higher than in the analogous 3 (135 and 145 Hz), suggesting that the SiH donor site *trans* to P in 5 is exerting weaker *trans*-influence than a phosphine donor in 3. The SiH hydride in 5 resonated at δ −5.32 ppm as a doublet of doublets with satellites from additional coupling to ^{29}Si (J_{Rh-H} = 37 Hz, $^2J_{P-H}$ = 19 Hz, $^1J_{Si-H}$ = 110 Hz).

In a series of reactions, NMR tube solutions of 5 in C_6D_6 were treated with various phosphites in a 1 : 1 ratio. These reactions resulted in the displacement of free COE and the formation of phosphite adducts 6–10. They were identified based on the presence (in each case) of two $^{31}P\{^1H\}$ NMR resonances of equal intensity coupled to each other (and to ^{103}Rh), as a well as a single hydride resonance displaying the diagnostic ddd multiplicity from coupling to two different ^{31}P nuclei and a ^{103}Rh nucleus, with additional satellites from coupling to ^{29}Si. Compounds 6–10 proved to be unstable on the timescale of experimental handling at ambient temperature, generating new unidentified compounds in solution. However, this degradation did not generate new hydride resonances.

Table 1 summarizes the relevant NMR data for 6–10. Surprisingly, the series of phosphites complexes appears to be split into two groups: Type A (6 and 7) with the hydride chemical shift around −4.6 ppm and Type B with the hydride chemical shifts at around −7.0···−7.5 ppm (8–10). On the balance of the data, 5 fits with the Type A phosphite adducts. The J_{Si-H} values for both types are consistent with substantial residual Si–H bonding, *i.e.*, an Si–H σ-complex, not a silyl/hydride structure.[1,2,3] The parent ligand 4 possesses a J_{Si-H} = 183 Hz.[16] The J_{Si-H} values are larger for Type A, suggesting greater disruption of the Si–H bond *vs.* Type B. The J_{Si-H} value for 5 can be compared with that for the SiNN analog 1 (51 Hz), based on which it appears that the Si–H bond in 1 is disrupted to a more significant degree. This may be related to the lesser *trans*-influence of N (in 1) vs P (in 5) *trans* to Si–H permitting a closer Type B interaction. The ^{31}P and ^{29}Si NMR chemical shifts also approximately cluster into two groups for Type A or B.

Cooling a sample of 5 in toluene-d_8 to −65 °C resulted in a modest change in chemical shift from −5.3 to *ca.* −5.7 ppm for the now slightly broadened Si–H resonance. While this could be owing to a temperature-dependent rapid equilibrium between Type A and B conformers shifting towards a higher Type B proportion, the magnitude of the change is small and may simply reflect a temperature dependence of the chemical shift for Type A. Analysis of solutions of 6–10 by IR spectroscopy did not prove informative in distinguishing Type A and Type B forms.

Complexes of $P(OPh)_3$ (6) and $P(O^iPr_3)$ (7) are both of Type A, yet there is more electronic difference between them than between the trialkylphosphites found in Type B (8–10) and $P(O^iPr_3)$ (7). We tentatively conclude that the difference between the two types has a steric origin; with only the smallest tris(*n*-alkoxy)-substituted phosphites permitting Type B (Tolman cone angle values[20] given in Table 1).

Table 1 Summary of selected NMR data for compounds 6–10

#, Type, Θ[a]	δ, ^{31}P NMR[b]	δ, ^1H NMR[c]	δ, ^{29}Si NMR[d]	$^1J_{Rh-H}$, Hz	$^2J_{P'-H}$ [e], Hz	$^2J_{P-H}$ [f], Hz	$^1J_{Si-H}$, Hz
5 (A)	64.0 (193, –)	−5.32	14.7	19	–	37	110
6 (A) *121*	67.7 (171, 46)	−4.63	25.1	19	22	36	91
7 (A) *114*	66.0 (180, 45)	−4.64	21.2	19	21	35	93
8 (B) *110*	55.6 (152, 46)	−7.02	32.1	23	23	48	76
9 (B) *109*	54.9 (159, 42)	−7.24	32.0	20	26	48	76
10 (B) *107*	54.7 (150, 44)	−7.45	33.3	22	26	48	73

[a] Numbers in italic underneath compound numbers are Tolman's cone angle values;[20] the value for $P(OCH_2CH_2Cl)_3$ used for $P(O^nBu)_3$. [b] ^{31}P NMR chemical shift for the SiNP phosphorus, in ppm, and values in Hz for $^1J_{P-Rh}$ and $^2J_{P-P'}$. [c] ^1H NMR chemical shift for the Si–H, in ppm. [d] ^{29}Si shifts obtained from [^1H–^{29}Si] HSQC NMR analysis. [e] P′ refers to the phosphorus in $P(OR)_3$. [f] P refers to the SiNP phosphorus.

XRD and DFT structural studies

We were able to obtain single crystals of 6 and 10, whose solid-state structures were determined by X-ray diffractometry (Fig. 2). Both can be viewed as having a square-planar geometry about the Rh center, with the same donor sites. Nonetheless, there is an easily discernible difference between the orientation of the –Si^{i}Pr$_2$H group in the two structures. In the structure of 6, the hydrogen atom of Si–H is only 0.08(5) Å removed from the plane defined by the Si/Rh/P′ atoms, whereas in 10, the Si-bound H atom is removed from that plane by 0.88(4) Å. The Si–H vector in 6 is essentially in the same plane as the N/P/P′/Rh atoms, but in 10 it is nearly perpendicular. In addition, there is a dramatic difference in the Rh–Si distances (*ca.* 2.45 Å in 10 and *ca.* 2.79 Å in 6). It could also be noted that the Rh–P bond in 10 is *ca.* 0.04 Å longer than in 6. This is consistent with the smaller $^{1}J_{P\text{–}Rh}$ value in 10 and Type B compounds in general.

In order to better understand the structural distinction between Type A and Type B, we turned to the DFT methods (see ESI for method description†). Optimization of the structures 6 resulted in a structure that qualitatively resembles the XRD structure in that the SiH unit is "in-plane" and the Si atom is relatively distant from Rh. Optimization of 5 and 10 also led to what we view as Type A structures: "in-plane" Si–H and a long Rh–Si distance. This was in contrast to the XRD structure of 10, which we classify as Type B. It is likely that the difference in energy between Type A and B structures is small and DFT optimization may not capture this difference correctly. To obtain a computed Type B structure, we performed the optimization of 10 while restricting the positions of Rh/H/Si to where they were found in the XRD determination. Not surprisingly, this resulted in a conformation of the SiNP ligand that is quite similar to that found in the X-ray structure of 10. The Rh–P distance in 10-B was not restricted and was calculated to be longer than in the DFT-optimized structures 6-A and 10-A. This trend in the DFT-calculated structures qualitatively matches the comparison in the X-ray structures of 6 (Type A, shorter Rh–P) and 10 (Type B, longer Rh–P). The hydride ^{1}H NMR chemical shifts in the structures of 5-A, 6-A, 10-A, and 10-B were calculated (Fig. 3). The distinct value for 10-B corroborates the experimental dichotomy between Type A and Type B ^{1}H NMR chemical shifts for the SiH (Table 1). Notably, the Rh–Si distance in 10-B is similar, but slightly longer than that in 1 (*ca.* 2.38 Å), while the calculated Rh–Si distance in 5-A is much longer.

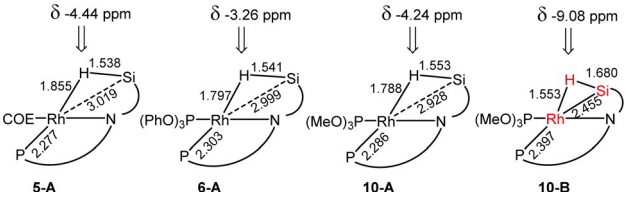

Fig. 3 Key interatomic distances and ^{1}H NMR chemical shifts for SiH in the DFT-calculated structures of 5-A, 6-A, 10-A, and 10-B. The atoms whose positions were restricted in the optimization of 10-B are shown in red.

All in all, Type B can be viewed as a structure that is best described as an Si–H σ-complex, with a relatively close approach of Si to Rh. In contrast, Type A can be viewed as a structure without a close approach between Rh and Si, where the hydride bridges these two atoms. The Type B interaction between Rh and SiH appears to be "tighter" as evidenced by the more negative ^{1}H NMR chemical shift and by the greater *trans*-influence on the P donor *trans* to SiH. Since the Type B interaction brings Si (and its ^{i}Pr substituents) closer to Rh, it makes sense that Type B is experimentally disfavoured by bulkier phosphites.

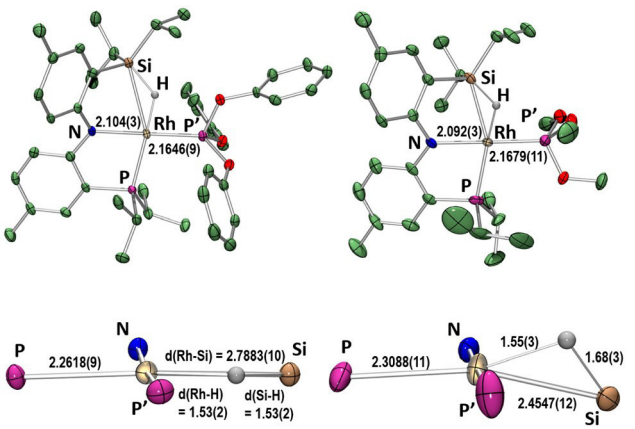

Fig. 2 ORTEP drawings (50% probability ellipsoids) of 6 (left) and 10 (right). Selected atom labelling is shown (except for C = green and O = red). The hydrogen atoms except for SiH are omitted for clarity in the top view and only one of the two crystallographically independent molecules of 10 is shown. The bottom view shows only the immediate coordination sphere about Rh in 6 and 10.

Conclusions

In conclusion, we have synthesized a series of square-planar, monovalent complexes (SiNP)Rh-L (5–10) supported by the SiNP pincer ligand. The Si–H unit in SiNP can interact in two distinct ways with Rh, ostensibly depending on the steric profile of the monodentate L (cyclooctene or phosphite) positioned *trans* to N. With smaller phosphites P(OR)$_3$ (R = ^{n}Bu, Et, or Me; 8–10), the Si atom approaches Rh more closely and the interaction can be described as an Si–H σ-complex. With larger phosphites (R = Ph or ^{i}Pr; 6 or 7) or L = COE (5) the Si atom is much more distant from Rh and the interaction is best described as an H bridging between Si and Rh. A more tightly bound Si–H in Type B possesses stronger *trans*-influence, and is paired with a longer Rh–P bond *trans* to it. Thus, counterintuitively, binding a larger phosphite (P′) leads to a shorter Rh–P bond within the SiNP pincer. This observation may have a bearing on the design of polydentate ligands containing Si–H moieties and the structural subtleties of their transition metal complexes.

Experimental

General considerations

Unless otherwise stated, all experiments were carried out using standard glovebox and Schlenk line techniques under a dry argon atmosphere. C_6D_6 was dried over NaK, benzophenone, and 18-crown-6, distilled, and stored over molecular sieves in an argon glovebox prior to usage. Diethyl ether, pentane, toluene, and tetrahydrofuran (THF) were dried and deoxygenated using a column solvent purification system. Fluorobenzene was dried over CaH_2 and distilled. All other deuterated solvents were degassed and stored over molecular sieves in an argon-filled glovebox. (SiNP)H (4)[16] and $[(COE)RhCl]_2$[21] were synthesized using reported literature procedures. All other chemical reagents were purchased from commercial suppliers and were used as received. 1D NMR spectra were recorded on Varian iNova 500 ($^{31}P\{^1H\}$ NMR, 202.276 MHz; $^{13}C\{^1H\}$ NMR, 125.670 MHz; ^1H NMR, 499.678 MHz), Bruker ARX-400 ($^{31}P\{^1H\}$ NMR, 161.976 MHz; $^{13}C\{^1H\}$ NMR, 100.613 MHz; ^1H NMR, 400.130), and JEOL ECX 400 spectrometers in given solvents. [^1H, ^{29}Si] HSQC NMR spectra were recorded on a Varian VnmrS 500 NMR spectrometer. Chemical shifts are reported in ppm (δ). $^{31}P\{^1H\}$ NMR spectra were referenced externally to an 85% phosphoric acid standard at δ 0 ppm.$^{13}C\{^1H\}$ and ^1H NMR spectra were internally referenced to residual solvent resonances. [^1H, ^{29}Si] HSQC NMR spectra were referenced externally to TMS at δ 0 ppm. In reporting spectral data, the following abbreviations were utilized: s = singlet; d = doublet; t = triplet; dd = doublet of doublets; m = multiplet; br = broad. Elemental analyses were performed by CALI, Inc. (Highland Park, NJ, USA).

(SiNP^H)Rh(COE) (5). To a 20 mL scintillation vial equipped with a magnetic stir bar was added $[(COE)_2Rh(Cl)]_2$ (132 mg, 0.18 mmol) and 3 mL fluorobenzene, forming an orange suspension. To this stirring suspension was added 3 mL of a separately prepared, yellow fluorobenzene solution of $NaN(SiMe_3)_2$ (70 mg, 0.38 mmol) and (SiNP)H (4) (159 mg, 0.37 mmol) causing an immediate color change to a dark red solution with notable formation of a precipitate (presumed to be NaCl). The mixture was allowed to stir for 30 min and was then filtered through a plug of Celite and silica. The resulting dark red solution was then dried *in vacuo* and the reddish-orange residue was washed with diethyl ether (3 × 2 mL) and dried under reduced pressure to provide the product as a free-flowing, bright orange solid. Yield: 118 mg (50%).^1H NMR (500 MHz, C_6D_6): δ 7.36 (dd $^3J_{H-H}$ = 4.5, 6.5 Hz, 1H, Ar–H), 7.34 (d, $^3J_{H-H}$ = 8 Hz, 1H, Ar–H), 7.07 (d, $^3J_{H-H}$ = 2 Hz, 1H, Ar–H), 6.83 (dd, $^3J_{H-H}$ = 8.5, 2 Hz, 1 H, Ar–H), 6.74 (d, $^3J_{H-H}$ = 8.5 Hz 1H, Ar–H), 6.71 (d, $^3J_{H-H}$ = 8 Hz, 1H, Ar–H), 3.30 (s, 2H, alkenyl-*H*), 2.49 (br, 1H), 2.37 (s, 1H), 2.18 (s, 3H, Ar–CH_3), 2.12 (s, 3H, Ar–CH_3), 1.98 (pentet, 2H), 1.82 (br, 2H), 1.62 (br, 6H), 1.47 (br, 5H), 1.23 (br, 9H), 1.01 (br, 3H), 0.96 (br, 3H), 0.81 (br, 3H), −5.32 (dd, $^2J_{P-H}$ = 37 Hz, $^1J_{Rh-H}$ = 19 Hz, $^1J_{Si-H}$ = 110 Hz, 1H, Rh–H(Si)). $^{13}C\{^1H\}$ NMR (128 MHz, C_6D_6): δ 164.9 (d, J_{P-C} = 22.6 Hz, P-ring C–N), 164.2 (Si-ring C–N), 135.5, 132.9, 131.7, 130.5, 126.5, 124.1, 123.7 (d, J_{P-C} = 6.6 Hz, P-ring C–H), 119.7 (d, J_{P-C} = 43.4 Hz, P-ring), 118.5, 116.6 (d, J_{P-C} = 12.4 Hz, P-ring), 62.5 (br), 59.6 (br), 35.8, 34.6, 32.0, 26.9, 22.4, 20.9, 20.6, 19.1 (m), 17.9, 16.6. $^{31}P\{^1H\}$ NMR (202 MHz, C_6D_6): δ 64.0 (d, $^1J_{Rh-P}$ = 193 Hz). ^{29}Si–^1H HSQC NMR (99 MHz, C_6D_6): δ 14.7. Elem. Anal. Calc. (found): C, 63.83(63.65); H, 8.67(8.51).

(SiNP)Rh($P(OPh)_3$) (6). To a J. Young tube was added 5 (20 mg, 0.03 mmol) and C_6D_6, forming a light orange solution. To this solution was added triphenyl phosphite (7 μL, 0.03 mmol) causing an immediate color change to a red solution. The J. Young tube was inverted several times and NMR spectra were collected indicating full conversion to the desired product. Red, single crystals suitable for X-ray diffractometry were grown from a saturated solution of pentane and hexane. ^1H NMR (400 MHz, C_6D_6): δ 7.53 (m, 7H, overlapping SiNP-Ar-CH and $P(OC_6H_5)_3$), 7.47 (d, $^3J_{H-H}$ = 8.3 Hz, 1H, Ar–H), 7.20 (d, $^3J_{H-H}$ = 2.0 Hz, 1H, Ar–H), 6.93 (m, 6H, $P(OC_6H_5)_3$), 6.85 (m, 3H), 6.77 (m, 3H), 2.22 (s, 3H, Ar–CH_3), 2.17 (s, 3H, Ar–CH_3), 2.16 (m, 2H), 1.56 (m, 2H), 1.41 (d, $^3J_{H-H}$ = 7.2 Hz, 6H, Si–^{i}Pr), 1.35 (dd, $^2J_{H-P}$ = 16.6, $^3J_{H-H}$ = 7.1 Hz, 6H, P–^{i}Pr), 1.23 (d, $^3J_{H-H}$ = 7.2 Hz, 6H, Si–^{i}Pr), 1.01 (dd, $^2J_{H-P}$ = 14.6, $^3J_{H-P}$ = 6.9 Hz, 6H, P–^{i}Pr), −4.63 (ddd, *trans* $^2J_{P-H}$ = 36 Hz, *cis* $^2J_{P-H}$ = 22 Hz, $^1J_{Rh-H}$ = 19 Hz, $^1J_{Si-H}$ = 91 Hz, Rh–H (Si))). $^{13}C\{^1H\}$ NMR (100 MHz, C_6D_6): δ 164.3 (P-ring C–N), 164.5 (Si-ring C–N), 152.5 (d, J_{P-C} = 7.0 Hz), 135.3, 132.9, 131.4, 129.6, 126.2, 123.3 (d, J_{P-C} = 6.6 Hz), 120.9 (d, J_{P-C} = 6.3 Hz), 35.9, 30.3 (d, J_{P-C} = 1.4 Hz), 27.0, 25.8, 20.8 (d, J_{P-C} = 30.7 Hz), 19.9, 18.9, 18.8, 17.5. $^{31}P\{^1H\}$ NMR (162 MHz, C_6D_6): δ 128.0 (dd, $^1J_{Rh-P}$ = 248.6 Hz, $^2J_{P-P}$ = 46.0 Hz, $P(OPh)_3$), 67.7 (dd, $^1J_{Rh-P}$ = 171.0 Hz, $^2J_{P-P}$ = 46.0 Hz, SiNP). ^{29}Si–^1H HSQC NMR (99 MHz, C_6D_6): δ 25.1.

(SiNP)Rh($P(O^iPr)_3$) (7). To a J. Young tube was added 5 (30 mg, 0.05 mmol) and C_6D_6, forming a light orange solution. To this solution was added triisopropyl phosphite (12 μL, 0.05 mmol) causing an immediate color change to a red solution. The J. Young tube was inverted several times and NMR spectra were collected indicating full conversion to the desired product. ^1H NMR (400 MHz, C_6D_6): δ 7.62 (dd, *J* = 8.6, 4.2 Hz, 1H, Ar–H), 7.50 (d, *J* = 8.3 Hz, 1H, Ar–H), 7.32 (d, *J* = 1.8 Hz, 1H, Ar–H), 7.09 (dd, *J* = 7.7, 1.5 Hz, 1H, Ar–H), 6.84 (m, 2H, 2 overlapping Ar–H), 4.73 (m, 3H, $P(OCHMe_2)_3$), 2.54 (m, 2H), 2.25 (s, 3H, Ar–CH_3), 2.24 (s, 3H, Ar–CH_3), 1.76 (m, 2H), 1.47 (d, $^3J_{H-H}$ = 7.4 Hz, 6H, Si–^{i}Pr), 1.40 (d, $^3J_{H-H}$ = 7.4 Hz, 6H, Si–^{i}Pr), 1.39 (dd, $^2J_{H-P}$ = 16.7 Hz, $^3J_{H-H}$ = 6.9 Hz, 6H, P–^{i}Pr), 1.26 (dd, $^2J_{H-P}$ = 14.0 Hz, $^3J_{H-H}$ = 7.0 Hz, 6H, P–^{i}Pr), 1.18 (d, *J* = 6.1 Hz, 18H, $P(OCHMe_2)_3$), −4.64 (ddd, *trans* $^2J_{P-H}$ = 35 Hz, *cis* $^2J_{P-H}$ = 21 Hz, $^1J_{Rh-H}$ = 19 Hz, $^1J_{Si-H}$ = 93 Hz, Rh–H(Si))). $^{13}C\{^1H\}$ NMR (100 MHz, C_6D_6): δ 164.6 (d, J_{P-C} = 1.6 Hz, Si-ring C–N), 163.7 (dd, J_{P-C} = 20.4, 3.0 Hz, P-ring C–N), 135.0, 132.5 (d, J_{P-C} = 1.9 Hz), 131.9, 131.3, 125.6, 122.4 (d, J_{P-C} = 6.2 Hz), 121.7 (d, J_{P-C} = 37.8 Hz), 119.0 (d, J_{P-C} = 2.8 Hz), 116.2 (d, J_{P-C} = 11.7 Hz), 68.2 (d, J_{P-C} = 2.1 Hz, $P(OCHMe_2)$, 26.1, 24.9 (d, J_{P-C} = 3.4 Hz), 24.6 (d, J_{P-C} = 4.1 Hz), 21.0, 20.7, 20.5, 20.3 (d, J_{P-C} = 5.5 Hz), 20.0, 18.5, 15.2. $^{31}P\{^1H\}$ NMR (162 MHz, C_6D_6): δ 144.5 (dd, $^1J_{Rh-P}$ = 226.0 Hz, $^2J_{P-P}$ = 46.0 Hz, $P(O^iPr)_3$), 66.0 (dd, $^1J_{Rh-H}$ = 180.0 Hz, $^2J_{P-P}$ = 46.0 Hz, SiNP). ^{29}Si–^1H HSQC NMR (99 MHz, C_6D_6): δ 21.2.

(SiNP)Rh(P(OBu)$_3$) (8). To a J. Young tube was added 5 (30 mg, 0.05 mmol) and C_6D_6, forming a light orange solution. To this solution was added tributyl phosphite (13 μL, 0.05 mmol) causing an immediate color change to a red solution. The J. Young tube was inverted several times and NMR spectra were collected indicating full conversion to the desired product. ^{1}H NMR (400 MHz, C_6D_6): δ 7.73 (dd, J = 8.5, 4.3 Hz, 1H, Ar–H), 7.63 (d, J = 8.3 Hz, 1H, Ar–H), 7.32 (br, 1H, Ar–H), 7.00 (d, J = 7.9 Hz, 1H, Ar–H), 6.85 (dd, J = 16.8, 8.4 Hz, 1H, Ar–H), 3.95(dt, $^3J_{P\text{–}H}$ = 6.0 Hz, $^3J_{H\text{–}H}$ = 6.0 Hz, 6H, (P(OCH$_2$CH$_2$CH$_2$CH$_3$)$_3$), 2.52 (m, 2H), 2.31 (s, 3H, Ar–CH$_3$), 2.23 (s, 3H, Ar–CH$_3$), 1.79 (m, 2H), 1.49 (m, 12H, overlapping P–^{i}Pr (6H) and P(OBu)$_3$ (6H) resonances), 1.42 (d, J = 7.0 Hz, 6H, Si–^{i}Pr), 1.36 (d, J = 7.1 Hz, 6H, Si–^{i}Pr), 1.28 (br q, J = 7.4 Hz, 6H, P(OCH$_2$CH$_2$CH$_2$CH$_3$)$_3$), 1.21 (dd, J = 13.9, 6.8 Hz, 6H, P–^{i}Pr), 0.82 (t, J = 7.4 Hz, 9H, (P(OCH$_2$CH$_2$CH$_2$CH$_3$)$_3$), −7.02 (ddd, *trans* $^2J_{P\text{–}H}$ = 48 Hz, *cis* $^2J_{P\text{–}H}$ = 23 Hz, $^1J_{Rh\text{–}H}$ = 23 Hz, $^1J_{Si\text{–}H}$ = 76 Hz, 1H, Rh–H(Si))). ^{13}C{^{1}H} NMR (100 MHz, C_6D_6): δ 164.8 (br, P-ring C–N), 164.6 (br, Si-ring C–N), 135.0, 132.8, 132.3, 130.4, 130.0, 126.8, 122.3 (d, $J_{P\text{–}C}$ = 4.9 Hz, P-ring), 119.8, 118.9 (d, $J_{P\text{–}C}$ = 37.2 Hz, P-ring), 114.9 (d, $J_{P\text{–}C}$ = 13.6 Hz, P-ring), 64.0 (P(OCH$_2$CH$_2$CH$_2$CH$_3$)), 32.9, 25.4 (d, J = 23.9 Hz), 21.1, 20.6, 20.2, 19.8 (d, J = 5.6 Hz), 19.7, 19.6, 18.2, 16.1, 14.0. ^{31}P{^{1}H} NMR (162 MHz, C_6D_6): δ 145.0 (dd, $^1J_{Rh\text{–}P}$ = 220.8 Hz, $^2J_{P\text{–}P}$ = 46 Hz, Rh–P(OBu$_3$)), 55.6 (dd, $^1J_{Rh\text{–}P}$ = 151.9 Hz, $^2J_{P\text{–}P}$ = 46 Hz, ^{iPr}SiNP). ^{29}Si–^{1}H HSQC NMR (99 MHz, C_6D_6): δ 32.1.

(SiNP)Rh(P(OEt)$_3$) (9). To a J. Young tube was added 5 (29 mg, 0.05 mmol) and C_6D_6, forming a light orange solution. To this solution was added triethyl phosphite (8 μL, 0.05 mmol) causing an immediate color change to a red solution. The J. Young tube was inverted several times and NMR spectra were collected indicating full conversion to the desired product. ^{1}H NMR (400 MHz, C_6D_6): δ 7.73 (dd, J = 8.6, 4.4 Hz, 1H), 7.64 (d, J = 8.3 Hz, 1H), 7.31 (s, 3H), 6.99 (d, J = 7.7 Hz, 1H), 6.88 (dd, J = 8.3, 1.5 Hz, 1H), 6.82 (d, J = 8.7 Hz, 1H), 3.86 (dq, J = 6.9, 6.9 Hz, P(OCH$_2$CH$_3$)$_3$), 2.45 (m, 2H), 2.31 (s, 3H, Ar–CH$_3$), 2.23 (s, 3H, Ar–CH$_3$), 1.73 (m, 2H), 1.45 (d, J = 7.3 Hz, 6H, Si–^{i}Pr), 1.37 (dd, J = 16.6, 7.1 Hz, 6H, P–^{i}Pr), 1.33 (d, J = 7.3 Hz, 6H, Si–^{i}Pr), 1.17 (dd, J = 14.0, 6.9 Hz, 6H, P–^{i}Pr), 1.03 (t, J = 6.9 Hz, 9H, P(OCH$_2$CH$_3$)$_3$), −7.24 (ddd, *trans* $^2J_{P\text{–}H}$ = 48 Hz, *cis* $^2J_{P\text{–}H}$ = 26 Hz, $^1J_{Rh\text{–}H}$ = 20 Hz, $^1J_{Si\text{–}H}$ = 76 Hz, 1H, Rh–H(Si))). ^{13}C{^{1}H} NMR (100 MHz, C_6D_6): δ 164.8 (d, $J_{P\text{–}C}$ = 1.8 Hz, P-ring C–N), 164.6 (Si-ring C–N), 135.0, 132.8, 132.2, 130.3, 130.0, 126.8, 122.2 (d $J_{P\text{–}C}$ = 6.0 Hz), 119.6, 119.0 (d, $J_{P\text{–}C}$ = 38.0 Hz), 114.9 (d, $J_{P\text{–}C}$ = 12.1 Hz), 59.9 (P(OCH$_2$CH$_3$)$_3$), 25.3 (d, $J_{P\text{–}C}$ = 24.0 Hz), 20.8, 20.6, 20.1, 19.8 (d, $J_{P\text{–}C}$ = 6.0 Hz), 19.6, 18.2, 16.2, 16.1. ^{31}P{^{1}H} NMR (162 MHz, C_6D_6): δ 145.4 (dd, $^1J_{Rh\text{–}P}$ = 221.2 Hz, $^2J_{P\text{–}P}$ = 42.0 Hz, P(OEt)$_3$), 54.9 (dd, $^1J_{Rh\text{–}P}$ = 158.6, $^2J_{P\text{–}P}$ = 42.0 Hz, SiNP). ^{29}Si–^{1}H HSQC NMR (99 MHz, C_6D_6): δ 32.0.

(SiNP)Rh(P(OMe)$_3$) (10). To a J. Young tube was added (SiNP)Rh(COE) (25 mg, 0.04 mmol) and C_6D_6, forming a light orange solution. To this solution was added trimethyl phosphite (5 μL, 0.04 mmol) causing an immediate color change to a red solution. The J. Young tube was inverted several times and NMR spectra were collected indicating full conversion to the desired product. Single crystals suitable for X-ray diffraction were grown through vapor transfer of hexamethyldisiloxane into an isooctane solution of 10. ^{1}H NMR (500 MHz, C_6D_6): δ 7.72 (dd, J = 8.7, 4.5 Hz, 1H), 7.63 (d, J = 8.3 Hz, 1H), 7.30 (d, J = 1.9 Hz, 1H), 6.94 (dd, J = 8.1, 1.4 Hz, 1H), 6.88 (dd, J = 8.3, 1.7 Hz, 1H), 6.82 (d, J = 8.7, Hz, 1H), 3.28 (d, J = 11.9 Hz, 9 H, P(OMe)$_3$), 2.37 (m, 2H), 2.31 (s, 3H, Ar–CH$_3$), 2.21 (s, 3H, Ar–CH$_3$), 1.72 (m, 2H), 1.40 (d, J = 7.3 Hz, 6H, Si–^{i}Pr), 1.33 (dd, J = 16.5, 7.0 Hz, 6H, P–^{i}Pr), 1.30 (d, J = 7.2 Hz, 6H, Si–^{i}Pr), 1.11 (dd, J = 14.1, 7.0 Hz, 6H, P–^{i}Pr), −7.45 (ddd, *trans* $^2J_{P\text{–}H}$ = 48 Hz, *cis* $^2J_{P\text{–}H}$ = 26 Hz, $^1J_{Rh\text{–}H}$ = 22 Hz, $^1J_{Si\text{–}H}$ = 73 Hz, 1H, Rh–H(Si))). ^{13}C{^{1}H} NMR (128 MHz, C_6D_6): δ 164.8 (d, $J_{P\text{–}C}$ = 23.6 Hz, P-ring C–N), 164.5 (Si-ring C–N), 135.0, 132.9, 132.2, 130.4, 129.9, 127.0, 122.3, 119.6, 118.6 (d, $J_{P\text{–}C}$ = 40.2 Hz, P-ring), 114.9 (d, $J_{P\text{–}C}$ = 11.2 Hz, P-ring), 50.5 (P(OMe)$_3$), 25.1 (d, $J_{P\text{–}C}$ = 22.6 Hz), 21.0, 20.8, 20.6, 19.9, 19.6, 18.1, 16.0. ^{31}P{^{1}H} NMR (202 MHz, C_6D_6): δ 151.9 (dd, $^1J_{Rh\text{–}P}$ = 221.6 Hz, $^2J_{P\text{–}P}$ = 44.0 Hz, Rh–P(OMe$_3$)), 54.7 (dd, $^1J_{Rh\text{–}P}$ = 149.6, $^2J_{P\text{–}P}$ = 44.0 Hz, ^{iPr}SiNP). ^{29}Si–^{1}H HSQC NMR (99 MHz, C_6D_6): δ 33.3.

Conflicts of interest

There are no conflicts to declare.

Acknowledgements

We are grateful to the US National Science Foundation for support of this research *via* grants CHE-1565923 and CHE-2102324 to O. V. O. (including AGEP-GRS supplements to A. J. K. and M. N. C.), and *via* grant CHE-1359175 supporting the REU site at Texas A&M (and the REU spell by B. M.). A. R. T. is thankful for the Cornell ACS section summer internship award. This work was also supported by State Key Laboratory of Urban Water Resource and Environment (Harbin Institute of Technology) (No. 2022TS36). Computer time made available by the National Supercomputing Center of China in Shenzhen (Shenzhen Cloud Computing Center) is gratefully acknowledged. We are grateful to Alexander Rono and Tenjing Sherpa for their assistance in the visualization of the structural data.

References

1 J. Y. Corey, *Chem. Rev.*, 2011, 111, 863–1071.
2 G. I. Nikonov, *Adv. Organomet. Chem.*, 2005, 53, 217–309.
3 G. Alcaraz and S. Sabo-Etienne, *Coord. Chem. Rev.*, 2008, 252, 2395–2409.
4 Y. Nakajima and S. Shimada, *RSC Adv.*, 2015, 5, 20603–20616.
5 J. V. Obligacion and P. J. Chirik, *Nat. Rev. Chem.*, 2018, 2, 15–34.
6 R. J. Hofmann, M. Vlatković and F. Wiesbrock, *Polymers*, 2017, 9, 534–570.

7 C. Cheng and J. F. Hartwig, *Chem. Rev.*, 2015, 115, 8946–8975.
8 (*a*) D. Morales-Morales and D. Jensen, *The Chemistry of Pincer Compounds*, Elsevier, Amsterdam, 2007; (*b*) G. Van Koten and D. Milstein, *Topics in Organometallic Chemistry*, Springer, Heidelberg, 2013, vol. 40, pp. 1–356; (*c*) K. J. Szabó and O. F. Wendt, *Pincer and Pincer-Type Complexes: Applications in Organic Synthesis and Catalysis*, John Wiley & Sons, Weinheim, 2014.
9 (*a*) A. Adhikary and H. Guan, *ACS Catal.*, 2015, 5, 6858–6873; (*b*) E. Poverenov and D. Milstein, *Top. Organomet. Chem.*, 2013, 40, 21–48; (*c*) J. Choi, A. H. R. MacArthur, M. Brookhart and A. S. Goldman, *Chem. Rev.*, 2011, 111, 1761–1779.
10 B. Ghaffari, S. M. Preshlock, D. L. Plattner, R. J. Staples, P. E. Maligres, S. W. Krska, R. E. Maleczka and M. R. Smith, *J. Am. Chem. Soc.*, 2014, 136, 14345–14348.
11 For pincer ligands with a central silyl unit arising from an Si–H containing precursor, see: (*a*) J. C. DeMott, W. Gu, B. J. McCulloch, D. E. Herbert, M. D. Goshert, J. R. Walensky, J. Zhou and O. V. Ozerov, *Organometallics*, 2015, 34, 3930–3933; (*b*) M. T. Whited, A. M. Deetz, J. W. Boerma, D. E. DeRosha and D. E. Janzen, *Organometallics*, 2014, 33, 5070–5073; (*c*) M. T. Whited, A. M. Deetz, T. M. Donnell and D. E. Janzen, *Dalton Trans.*, 2016, 45, 9758–9761; (*d*) M. T. Whited, J. Zhang, S. Ma, B. D. Nguyen and D. E. Janzen, *Dalton Trans.*, 2017, 46, 14757–14761; (*e*) E. E. Korshin, G. Leitus, L. J. W. Shimon, L. Konstantinovski and D. Milstein, *Inorg. Chem.*, 2008, 47, 7177–7189; (*f*) S. J. Mitton, R. McDonald and L. Turculet, *Organometallics*, 2009, 28, 5122–5136; (*g*) J. Takaya and N. Iwasawa, *J. Am. Chem. Soc.*, 2008, 130, 15254–15255; (*h*) J. Zhang, B. J. Foley, N. Bhuvanesh, J. Zhou, D. E. Janzen, M. T. Whited and O. V. Ozerov, *Organometallics*, 2018, 37, 3956–3962.
12 C.-I. Lee, J. Zhou and O. V. Ozerov, *J. Am. Chem. Soc.*, 2013, 135, 3560–3566.
13 J. Zhou, C.-I. Lee and O. V. Ozerov, *ACS Catal.*, 2018, 8, 536–545.
14 C.-I. Lee, N. A. Hirscher, J. Zhou, N. Bhuvanesh and O. V. Ozerov, *Organometallics*, 2015, 34, 3099–3102.
15 A closely related case of Rh and Ir complexes supported by a ligand combining a bipyridine with an appended Si–H side arms was reported very recently: T. Komuro, D. Mochizuki, H. Hashimoto and H. Tobita, *Dalton Trans.*, 2022, 51, 9983–9987.
16 C.-I. Lee, J. C. DeMott, C. J. Pell, A. Christopher, J. Zhou, N. Bhuvanesh and O. V. Ozerov, *Chem. Sci.*, 2015, 6, 6572–6582.
17 J. J. Davidson, J. C. DeMott, C. Douvris, C. M. Fafard, N. Bhuvanesh, C.-H. Chen, D. E. Herbert, C.-I. Lee, B. J. McCulloch, B. M. Foxman and O. V. Ozerov, *Inorg. Chem.*, 2015, 54, 2916–2935.
18 L. Fan, B. M. Foxman and O. V. Ozerov, *Organometallics*, 2004, 23, 326–328.
19 S. Gatard, C. Guo, B. M. Foxman and O. V. Ozerov, *Organometallics*, 2007, 26, 6066–6075.
20 C. A. Tolman, *J. Am. Chem. Soc.*, 1970, 92, 2956.
21 A. Van der Ent, A. L. Onderdelinden and R. A. Schunn, *Inorg. Synth.*, 1973, 14, 92–93.